

Command Shaping for Micro-Mills and CNC Controllers

Joel Fortgang*, William Singhose*, Juan de Juanes Márquez**, Jesus Pérez**

Abstract—Micro-milling requires both high speed and high accuracy in order to economically produce parts with features on the scale of 1 micron. Because micro-mills are small, they are more flexible than traditional large scale machines and therefore vibration is a problem. Since they also require high positioning precision, even small vibrations of the cutting tool are also an issue. This paper presents a nonlinear command shaping technique to reduce the vibrations of a micro-mill which can be implemented with a standard CNC controller. The robustness of this technique to modelling errors and disturbances is investigated. Theoretical proofs and experimental demonstrations of the command shaping technique are presented. The improved performance from the command shaping technique enables higher throughput and improved accuracy of the machine.

I. INTRODUCTION

The micro-milling machining operation allows parts to be created by physical cutting which have features on the scale of $1\mu m$. However, since the scale is much smaller than traditional milling, the stiffness from the cutting interface to ground can be significantly less. This lower stiffness can translate into machining error, or vibration that must be avoided by reducing process speed. Some of this flexibility comes from the mill's cutting tool, but the machine structure also contributes to this problem. Furthermore, due to the required precision of micro-mills, feedback controller flexibility can also be an issue.

While the stiffness of most micro-mills is large enough to counteract machining forces on the positioning system, the inertial forces from high-speed motion of the tool can cause the system to vibrate or deflect. Command shaping is an effective technique for dealing with these inertial forces. The fundamental principle is to cancel vibration from some part of the command with vibration from other parts of the command. The command shaping technique is often simple to implement, thereby allowing its use on existing numerical controllers.

A. Micro-Milling

Micro-mills have a wide range of applications including cutting materials that are highly reflective, as well as transparent, which are not machinable with lasers. Another advantage of micro-milling over other micro-manufacturing techniques is that it provides minimal tapering of the cut. These qualities lead to micro-milling applications for the creation of micromolds for injection molding [1], [2], microgears for watches, table top milling centers [3], masks for x-ray lithography [4], [5], and high precision lenses and

*Woodruff School of Mechanical Engineering, Georgia Institute of Technology, Atlanta, GA gt8520a@mail.gatech.edu, bill.singhose@me.gatech.edu

**Escuela Técnica Superior de Ingenieros Industriales, Madrid, Spain jmarquez@etsii.upm.es, jperez@dimf.etsii.upm.es

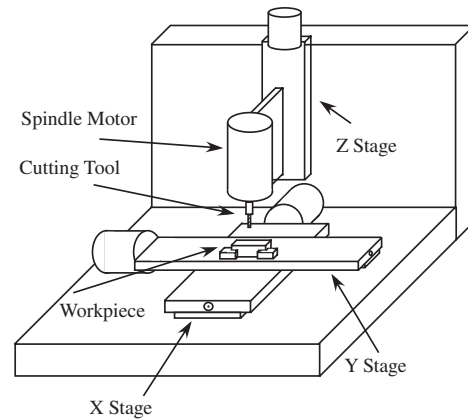


Fig. 1. Diagram of ETSII Micro-Mill.

gratings for optics [6], [7]. The cutter material can also vary from hard metal to single diamond chips used as pseudo ball-end mills [8], [9].

The throughput of micro-milling operations has been limited by the speed of the spindle. However, researchers have managed to push spindle speeds up to a few hundred thousand RPM [3]. With advancement in spindle speed it is theoretically possible to move the structure of the mill faster while maintaining cut quality and cutting force.

A high-speed micro-mill has been constructed at Escuela Técnica Superior de Ingenieros Industriales (ETSII) in Madrid, Spain [2]. The machine, diagramed in Figure 1, uses three identical precision linear stages driven by DC motors in the X, Y and Z directions with encoder resolutions of $0.5\mu m$. The X stage carries the Y Stage, while the Z stage controls the height of the tool spindle. The tool spindle is air and oil lubricated, as well as refrigerated in order to reach 120,000 RPM. The stage velocities are limited to $100\frac{mm}{s}$ with maximum accelerations of $1000\frac{mm}{s^2}$. A MM4006 Newport Motion Controller with PD feedback is used to control the trajectory of the stages. This controller is designed to produce complicated trajectory patterns in space but allows limited control over the time motion of the the tool. It lacks the ability to define the time at which changes in the position command occur.

B. Mill Response

The ETSII micro-mill uses bang-coast-bang acceleration profiles (trapezoidal velocities) to complete all of its moves. Of course, it does not track these trajectories exactly. For example, Figure 2 shows the tracking error for a bang-coast-bang acceleration trajectory with a maximum velocity of $24\frac{mm}{s}$ and an acceleration limit of $900\frac{mm}{s^2}$. Notice that the error from the desired trajectory can be more than $20\mu m$. This deviation from the desired trajectory is larger than the $1\mu m$ accuracy often desired in micro-milling. To characterize this tracking error, several variables can be

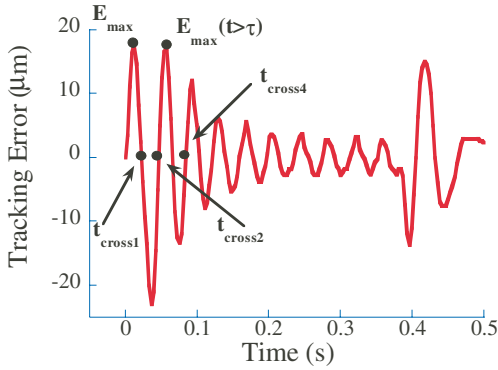


Fig. 2. Example Trajectory Error.

used, as shown in Figure 2. The magnitude of the error is quantified by both the maximum positive error, E_{max} , that occurs at the first peak in the error signal, and the peak after the acceleration pulse is over, $E_{max}(t > \tau)$, where τ is the length of the acceleration pulse. The oscillatory response of the mill is described by the crossing points where the error signal transitions between positive and negative. The second and fourth points, t_{cross2} and t_{cross4} , will be important crossing times used later to implement the command shaping scheme.

The effect of this deviation from the desired trajectory grows as part complexity increases. For a cut utilizing the motion of only one stage, the error from the desired trajectory can lead to an irregular surface finish and an increased force on the tool, because the cutting edge will oscillate only in the cut direction thus creating a varying feed-rate. However, if the trajectory is in multiple dimensions, then the error will lead to significant geometric variations thereby altering the gross dimensions of the part. The tool vibration will no longer be in line with the cut, and the previously mentioned problems of surface finish and forcing variations will be exacerbated.

The response of the machine is driven by the dynamics of the controller and the stages. As opposed to traditional milling, the cutting forces from micro-milling do not significantly alter the motion of the machine [2], [10]. Figure 3 shows the trajectory error for two motions of the tool, with and without cutting. The responses are virtually the same for both cases and well within the bounds of the machine's repeatability.

II. COMMAND SHAPING

Command shaping techniques change the input to the system in such a way as to minimize deflection and/or vibration. This is accomplished by having the vibration resulting from some components of the command interfere destructively with vibration induced by other components in the command. For example, consider an undamped second-order system given a unit impulse. The response to such an input, A_1 , is shown by the solid line in Figure 4. If another impulse of opposite magnitude, A_2 , is applied to the system at a later time, then the response is the dotted line. However, if both impulses are given to the system, then the resultant response has zero vibration after the second impulse. This

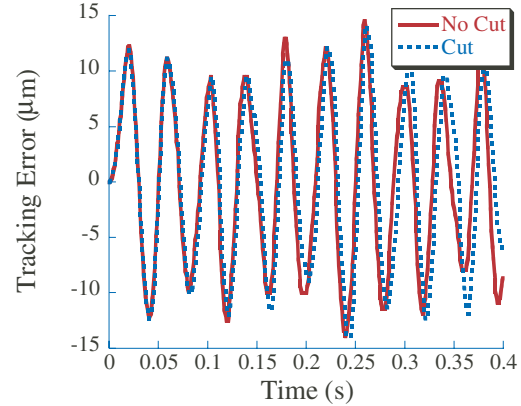


Fig. 3. Dynamic Effect of Cutting.

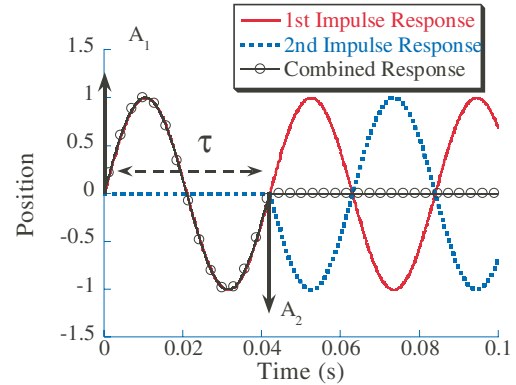


Fig. 4. Destructive Interference of Dynamic Response.

principle is used here to design acceleration profiles that cause minimal vibration in the system.

Driving a system with impulses is unrealistic. Therefore for a more reasonable bang-coast-bang acceleration profile, the vibration can be reduced by adjusting the acceleration to produce an input command with good vibration characteristics. The acceleration pulses can be viewed as the integral of two impulses, one positive and one negative. Therefore, if these component impulses can be designed correctly, then the corresponding pulse will induce little vibration. The use of the impulses instead of the pulse itself allows easier derivation. These impulses must be equal in magnitude for the input to be a pulse. Also, the magnitude of the pulses and the time spacing must combine to force the system to reach the appropriate feed-velocity, V . This relationship is defined by:

$$V = A\tau \quad (1)$$

If the values of A and τ are chosen correctly, then the vibration in the system can be minimized.

To find the values of A and τ to reach a desired velocity, consider a damped second-order response to an impulse of magnitude A_i at time t_i :

$$x(t) = \left[A_i \frac{\omega_n}{\sqrt{1 - \zeta^2}} e^{\zeta\omega_n(t-t_i)} \right] \sin(\omega_n \sqrt{1 - \zeta^2}(t - t_i)) \quad (2)$$

Where ω_n is the system's natural frequency and ζ is the

damping ratio. Assuming the system is linear and time invariant, superposition can be used to find the response to A_1 and A_2 , where $A_1 = A$ and $A_2 = -A$. For time greater than the time of the final impulse, τ , the response is:

$$x(t) = \left[A \frac{\omega_n}{\sqrt{1-\zeta^2}} e^{\zeta\omega_n t} \right] \sin(\omega_d t) + \left[A \frac{\omega_n}{\sqrt{1-\zeta^2}} e^{\zeta\omega_n(t-\tau)} \right] \sin(\omega_d(t-\tau)) \quad (3)$$

where the damped natural frequency is $\omega_d = \omega_n \sqrt{1-\zeta^2}$. This equation can then be used to find A and τ to yield a low level of vibration.

The following trigonometric identity can be used to simplify (3):

$$B_1 \sin(\alpha t + \phi_1) + B_2 \sin(\alpha t + \phi_2) = A_\Sigma \sin(\alpha t + \psi) \quad (4)$$

Where the amplitude A_Σ is:

$$A_\Sigma = \sqrt{\left(\sum_{j=1}^2 B_j \cos \phi_j \right)^2 + \left(\sum_{j=1}^2 B_j \sin \phi_j \right)^2} \quad (5)$$

and the B terms are:

$$B_1 = \frac{A\omega_n}{\sqrt{1-\zeta^2}} e^{-\zeta\omega_n t} \quad (6)$$

and

$$B_2 = \frac{A\omega_n}{\sqrt{1-\zeta^2}} e^{-\zeta\omega_n(t-\tau)} \quad (7)$$

The amplitude A_Σ of the boundary of the vibratory response $x(t)$ at any given time after τ can then be simplified, without having to calculate ϕ_1, ϕ_2 or ψ . This amplitude simplifies to:

$$A_\Sigma = \frac{\omega_d}{\sqrt{1-\zeta^2}} e^{-\zeta\omega\tau} \sqrt{(C(\omega_d, \zeta))^2 + (S(\omega_d, \zeta))^2} \quad (8)$$

Where

$$C(\omega_d, \zeta) = A(1 - e^{\zeta\omega_n\tau} \cos(\omega_d\tau)) \quad (9)$$

$$S(\omega_d, \zeta) = -Ae^{\zeta\omega_n\tau} \sin(\omega_d\tau) \quad (10)$$

Equation (8) is then used to determine the best command parameters. For the undamped case, A_Σ in (8) will be zero when τ is equal to integer multiples of the system period. For example, Figure 4 shows the solution when τ is one period of vibration. This result is important because the acceleration/actuator limits on the machine often prohibit the use of the solution of Figure 4 to reach the desired feed-velocity, and thus τ is set equal to two period of vibration.

If there is damping in the system, as is the case for any real micro-mill, then (8) can never be equal to zero, except for the trivial case of $\tau = 0$. However, significant vibration reduction is still possible, and the τ that minimizes (8) is approximately equal to integer multiples of the system period. The global minimum excluding the trivial case is given by

$$\tau = \frac{2\pi}{\omega_n} \quad (11)$$

while local minimum occur at every integer multiple of τ provided there is damping in the system.

The acceleration input to the system is then designed for a given feed-velocity with an acceleration duration of τ as defined by equation (11) and an acceleration given by

$$A = \frac{V}{n\tau} \quad (12)$$

where V is the desired feed-velocity, and n is the smallest positive integer such that $A \leq A_{limit}$ where A_{limit} is the maximum acceleration possible.

A. Physical Implementation

If the system's response is close to that of an under-damped second-order system, then the command shaping technique only needs a frequency measurement to determine τ . Simply look at the tracking error of the machine for the second zero crossing, t_{cross2} , which is ideally equal to τ . Once τ is known, then the technique described above can be used to determine the feed-acceleration and feed-velocity for a particular move to minimize vibration and these values can be sent to the controller. To restate, the only values that the controller needs to implement the command shaping technique are the acceleration, desired feed-velocity and t_{cross2} .

B. Nonlinearity Compensation

The proposed command shaping process is straight forward in its application to linear systems. However, like all real machines the ETSII micro-mill is nonlinear. This nonlinearity appears in the time response of the machine as a function of the acceleration. Unfortunately, t_{cross2} is not constant. The time at which the error goes to zero is dependent on the acceleration magnitude. This nonlinear effect complicates the trajectory design. This change in the crossing time could be dealt with by introducing a more robust command shaper [11], [12]. However, the motion controller of the ETSII milling machine and other commercial manufacturing machines is limited, and therefore requires a simple shaping scheme to be used. The solution advocated here is to adjust the command shaper parameters, namely τ , depending on the desired acceleration. This requires the command design scheme to consider the acceleration-induced nonlinearity. This process while simple to implement requires a thorough initial investigation of the machine.

Compensating for this nonlinearity in the zero crossing times by adjusting the command algorithm yields successful vibration reduction over all accelerations and therefore feed-rates. In order to solve for an appropriate command shaper, the relationship between all possible accelerations and the zero crossing times must be developed. Figure 5 shows how the second zero crossing time changes versus the acceleration of the X stage. If the mill behaved linearly, then the line would be horizontal. However, since the experimental data exponentially approaches the linear prediction, the experimental data will be used to find the command shaper. This is done with the following 3 steps:

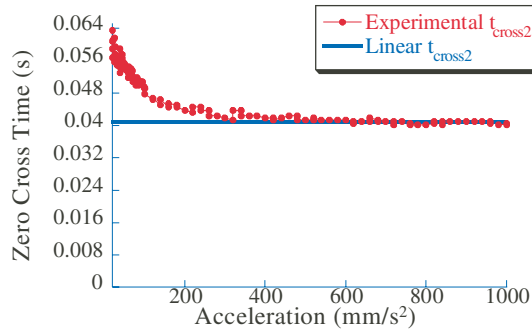


Fig. 5. Acceleration Dependence on t_{cross2} .

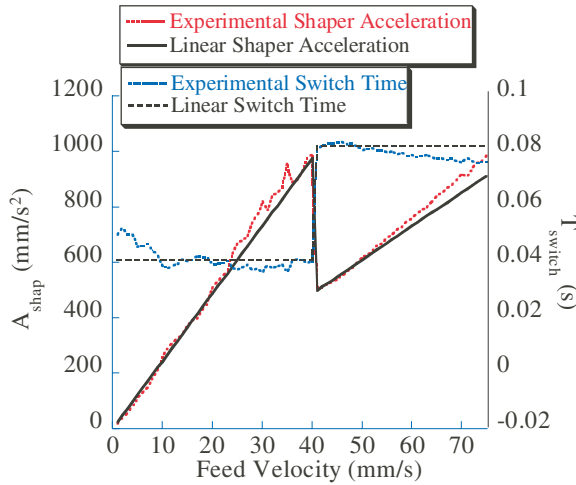


Fig. 6. Shaper Parameters.

- 1) Specify the desired feed-velocity.
- 2) Solve the vibration equation for all attainable accelerations.
- 3) Utilize the acceleration, A , where $\tau = \frac{V}{A}$ is closest to t_{cross2} .

This process produces a solution for the shaper at each desired feed-velocity. Figure 6 shows the command shaper's acceleration and duration over the feed-velocities attainable by the machine. In order to reduce the vibration at higher feed-velocities, the solution becomes bounded by actuator saturation. This causes the acceleration pulse duration to discontinuously increase by one period of vibration (note the jump at 40 mm/s). The linear case is also shown in Figure 6. The linear solution varies significantly from the nonlinear experimental data at low velocities, where the experimental switch time is 28% greater than the linear. This causes a deviation in the acceleration as well, but because of the scale it is not as noticeable in Figure 6. The solution also deviates from the linear at velocities around $35 \frac{mm}{s}$ and above $60 \frac{mm}{s}$ due to the effects of approaching the acceleration limits of the machine.

III. EXPERIMENTAL RESULTS

The above command design technique provides significant reduction of deviation from the desired trajectory. For example, Figure 7 shows the change in the following error of the machine for a move of 10mm at a feed-velocity

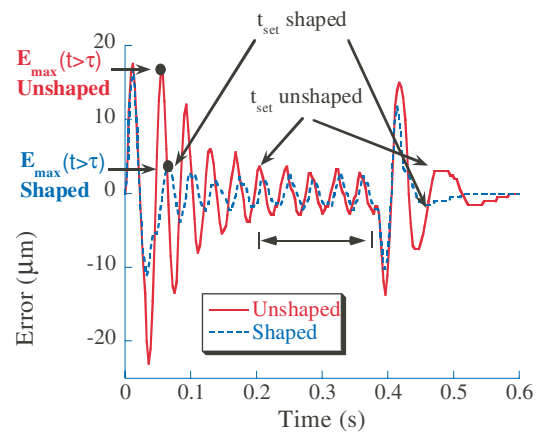


Fig. 7. Example Experimental Trajectory Error.

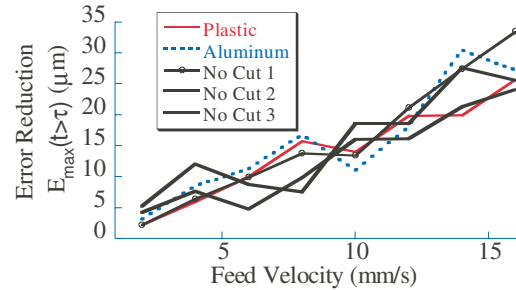


Fig. 8. Shaping Effectiveness With and Without Cutting.

of $26 \frac{mm}{s}$. The peak magnitude $E_{max}(t > \tau)$ after the acceleration pulse is reduced from $17.0 \mu m$ to $3.7 \mu m$, a reduction of 78%. While the previous discussion focused on the acceleration profile, by setting the trajectory parameters correctly, the vibration from the deceleration profile is also reduced. Also note, utilizing command generation improves the settling time of both the initial acceleration and the deceleration of the machine. A low level of vibration occurs in both cases.

A. Studies of Cutting Effects

Reducing the vibration of moves while not cutting is important. However, it is more important to improve the tracking during cutting operations. Because the cutting force's effect on the motion of the machine is small, the command generation technique also improves the trajectory following during cutting operations. Figure 8 compares the improvement in $E_{max}(t > \tau)$ with command generation for a variety of feed-velocities while cutting plastic and aluminum. By comparing these to the three cases where no cut was made, it can be seen that the variation between the cutting situations and the free moves are within the repeatability of the machine.

The results clearly show the effectiveness of the command generation scheme on the position of the stages. However, deflection of the cutting tool or other components not measured by the stage encoders could occur. To test if these deflections occurred, cuts with and without command generation were performed with a feed velocity of $28 \frac{mm}{s}$. Figure 9 shows a section of the stage responses after the acceleration period. The vibration amplitude is significantly

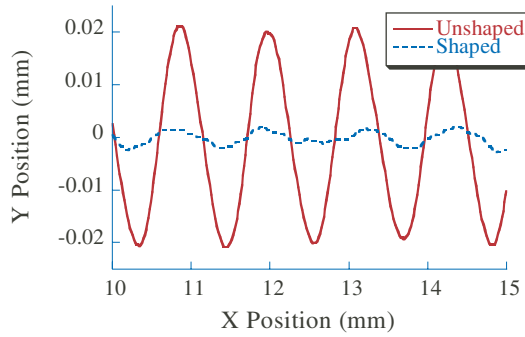


Fig. 9. Stage Response With and Without Command Shaping.

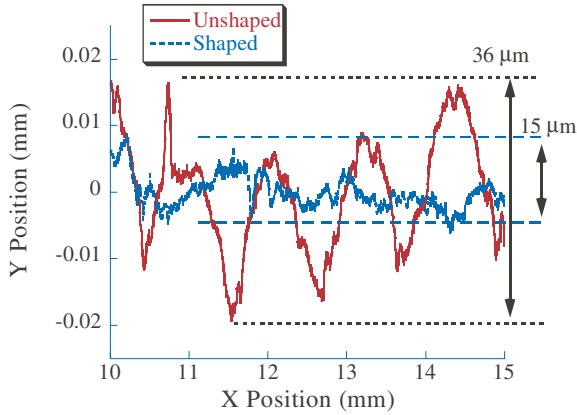


Fig. 10. Physical Part Surface With and Without Command Shaping.

lower in the case of shaping. The same vibration reduction can be seen in Figure 10 which is a measure of the actual surface dimensions of the machined material. The shaping reduces the variation along the actual surface from $36\mu\text{m}$ to $15\mu\text{m}$, a reduction of 58%. This data was obtained by photographing the machined surface using a microscope. While the command shaping improved the accuracy of the cut, it cannot reduce the small high frequency oscillations in the surface. These are due to the cutting dynamics of the mill and are beyond the capabilities of command shaping. The command shaping scheme applied here does not address tool runout, however command shaping can be tailored to reduce vibration of the tool itself if necessary.

A primary concern in micro-milling is limiting the forces in the cutting process to prevent cutting tool breakage. Therefore, any command scheme must not increase the existing forces on the tool. To measure this effect a Kistler Type 9256 C1 dynamometer was affixed to the Y stage and a series of experiments with and without command shaping were performed. Figure 11 shows how the maximum cutting forces both in line and normal to the cut direction are essentially unchanged with the use of command shaping.

IV. ROBUSTNESS INVESTIGATION

The command generation technique cannot provide zero vibration for cases where damping exists. It does, however provide significant vibration reduction for systems with low

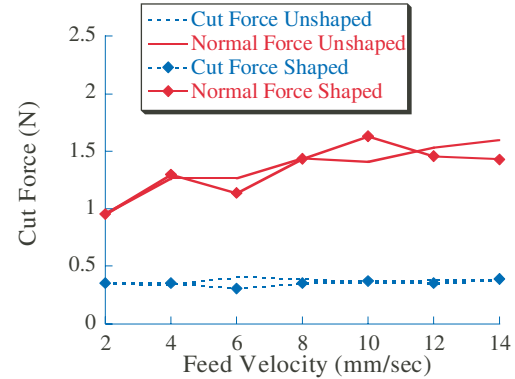


Fig. 11. Shaping Effect on Cutting Forces.

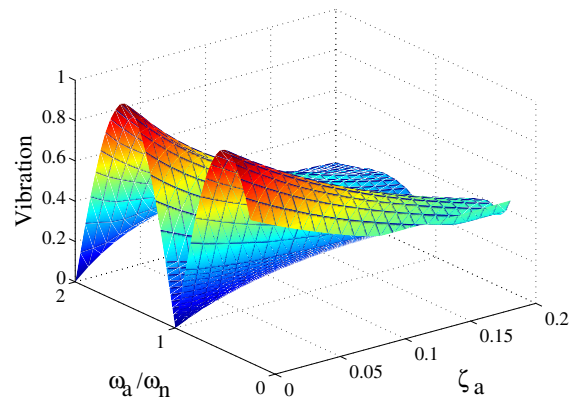


Fig. 12. Sensitivity to Damping and Frequency Error.

to moderate damping. Figure 12 shows how the theoretical performance of the command generation technique changes with errors in modelling of the natural frequency for different system damping ratios. The parameter $\frac{\omega_a}{\omega_m}$ represents the actual frequency divided by the modelled frequency, while ζ_a represents both the actual and the modelled damping ratio of the system.

Notice that with zero damping and perfect frequency modelling, vibration can theoretically be reduced to zero. As damping increases the resultant vibration also increases but remains below 20% of the maximum possible vibration for the damping range shown. The trough at the exact modelling frequency in Figure 12 represents a command designed using the solution to (11) which only deals with the undamped natural frequency. This is because the minimum of (8) is not strongly related to the damping ratio.

In terms of frequency modelling error, the curve in Figure 12 is steep in the frequency direction near exact modelling when damping is small. This means that the performance degrades quickly with modelling error in frequency.

Experimental tests were also made to study the effectiveness of the command shaping technique to changes in system frequency. Figure 13 shows the improvement in $E_{max}(t > \tau)$ (the maximum error after the initial acceleration pulse) with the use of command shaping for a variety of feed-velocities. Modelling error was induced by increasing the controller proportional gain from a baseline

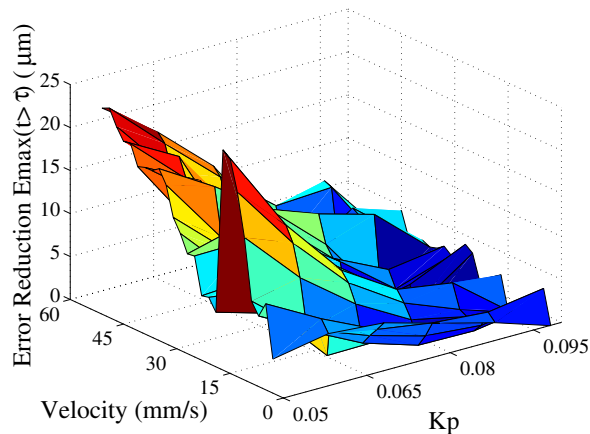


Fig. 13. Error Reduction with Frequency Modelling Error.

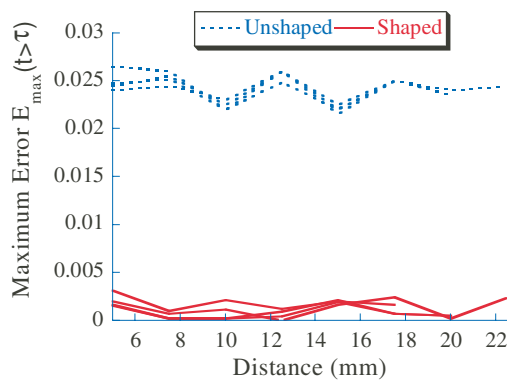


Fig. 14. External Forcing Effect.

of 0.05. The magnitude of the improvement drops rapidly as the controller gain deviates from the shaper designed value, as predicted by the theoretical results. Also, there is a discontinuity in the surface along the line of velocity at $40 \frac{mm}{s}$. This coincides with the abrupt jump in the value of τ to meet the actuator constraints. Similar results were found if modelling error exists in the damping or derivative gain of the system. This modelling error change in performance shows that while the command shaping technique is effective for reducing vibration over a wide variety of feed-velocities and damping, if the system cannot be modelled accurately in frequency, then the performance will suffer.

Another measure of robustness is the ability to cope with changes in cutting forces. Figure 8 showed that the system performed equally well with or without cutting. However, the magnitude of the cutting forces in Figure 8 was small - on the order of 1 Newton. Other micro-mills might encounter larger cutting forces, [13], [14] due to differing materials or cutting parameters like spindle speed, therefore the command shaping technique needs to be effective when larger forces are present. The larger forces must not alter the dynamics of the machine in such a way that the command shaping technique no longer functions correctly. This was tested by utilizing spring scales to apply a quantified disturbance force to the stages. Figure 14 shows the performance of the command shaping technique when three different springs were applied. The dashed lines show the maximum error without shaping when no spring and

three cases with springs where the spring applied 1.4, 3, and 12 N at the beginning of the moves and 2.4, 6.25, and 16 N at the end of the moves, respectively. The solid lines show the same no spring and three cases with springs for the shaped command. The results show that the maximum error after the acceleration pulse is the same even if larger forces were experienced than are typical in the operation of the ETSII micro-mill. From this it can be extrapolated that the command shaping technique should work on mills with larger cutting forces than the ETSII micro-mill.

V. CONCLUSIONS

A nonlinear command generation technique for choosing acceleration profiles based on the dynamic response allows a significant reduction in the tracking error of micro-mills, both with and without cutting. The application of this technique on micro-mills is successful because the magnitude of the cutting force is small enough not to significantly alter the dynamics. Finally, the command shaping technique allows increased accuracy, as well as the opportunity to increase the speed of the mill while maintaining existing accuracy, thus allowing a higher throughput.

REFERENCES

- [1] T. Kawai, K. Sawada, and Y. Takeuchi, "Ultra-precision micro structuring by means of mechanical machining," in *International Conference on MEMS*, 2001, pp. 22–25.
- [2] J. Fortgang, J. Marquez, and W. Singhose, "Application of command shaping on micro-mills," in *2004 Japan-USA Flexible Symposium on Automation*, Denver, CO, 2004.
- [3] Y. Okazaki, T. Mori, and N. Norita, "Desk-top nc milling machine with 200 krpm spindle," in *ASPE 2001 Annual Meeting*, Crystal City, VA, 2001, pp. 192–195.
- [4] C. R. Friedrich, P. Coane, J. Goettert, and N. Gopinathin, "Direct fabrication of deep x-ray lithography masks by micromechanical milling," *Precision Engineering*, vol. 22, pp. 164–173, 1998.
- [5] C. R. Friedrich and M. J. Vasile, "Development of the micromilling process for high-aspect-ratio microstructures," *Journal of Microelectromechanical Systems*, vol. 5, no. 1, pp. 33–38, 1996.
- [6] K. Sawada, S. Odaka, T. Kawai, T. Hirai, Y. Takeuchi, and T. Sata, "Manufacture of diffraction grating on tiny parts by means of ultraprecision milling," *Microsystem Technologies*, vol. 5, pp. 157–160, 1999.
- [7] K. Sawada, T. Kawai, T. Sata, and Y. Takeuchi, "Development of ultraprecision micro grooving (manufacture of v-shaped groove)," *JSME International Journal Series C*, vol. 43, no. 1, pp. 170–176, 2000.
- [8] Y. Takeuchi, K. Kato, S. Kawakita, K. Sawada, and T. Sata, "Generation of sculptured surfaces by means of an ultraprecision milling machine," *Annals of the CIRP*, vol. 41, no. 1, pp. 611–614, 1993.
- [9] Y. Takeuchi, K. Sawada, and T. Sata, "Ultraprecision 3d micromachining of glass," *Annals of the CIRP*, vol. 45, no. 1, pp. 401–404, 1996.
- [10] J. Fortgang, W. Singhose, J. Marquez, and J. Perez, "Cutting forces and dynamic effects of high speed micro-mills," *Submitted to Precision Engineering*.
- [11] W. Singhose, W. Seering, and N. Singer, "Residual vibration reduction using vector diagrams to generate shaped inputs," *J. of Mechanical Design*, vol. 116, no. June, pp. 654–659, 1994.
- [12] N. C. Singer and W. P. Seering, "Preshaping command inputs to reduce system vibration," *J. of Dynamic Sys., Measurement, and Control*, vol. 112, no. March, pp. 76–82, 1990.
- [13] W. Y. Bao and I. N. Tansel, "Modeling micro-end-milling operations. part i: analytical cutting force model," *International Journal of Machine Tools and Manufacture*, vol. 40, no. 15, pp. 2155–2173, 2000.
- [14] T. Dow, E. Miller, and K. Garrard, "Tool force and deflection compensation for small milling tools," *Precision Engineering*, vol. 28, pp. 31–45, 2004.